Invited Paper

Ultrafast carrier dynamics and laser action in ZnO nanowires

Marijn A.M. Versteegh*, Ruben E.C. van der Wel, Benjamin J.M. Brenny,
Bas Zegers, Wouter Ensing, and Jaap I. Dijkhuis

Debye Institute for Nanomaterials Science, Universiteit Utrecht,
P.O. Box 80000, 3508 TA Utrecht, The Netherlands

ABSTRACT

We have examined ultrafast carrier dynamics and light amplification in ZnO nanowires following subpicosecond excitation at room temperature. We performed time- and wavelength-resolved pump-probe transmission and gain measurements on a 'forest' of 100- to 500-nm thick and 20-μm long nanowires, epitaxially grown on a sapphire wafer. Measurements were done using 267-nm pump pulses for direct, but inhomogeneous excitation, and 800-nm pulses to achieve homogeneous excitation via three-photon absorption.

At the highest fluences, both for 267-nm and 800-nm pump pulses, a degenerate electron-hole plasma (EHP) is generated with carrier densities of 10^{25} m^{-3} or higher. We observed strong amplification of the probe, accompanied by a rapid decay (~ 1.5 ps) of the charge carriers. Below ~ 10^{25} m^{-3}, the EHP becomes non-degenerate and the decay much slower.

A dip in the pump-probe signal was observed, caused by ionization of probe exciton-polaritons by the pump. This effect allows for a measurement of the exciton-polariton dispersion relation and enhanced light-matter interaction in ZnO nanowires.

Keywords: ZnO nanowires, laser action, carrier dynamics, pump-probe, stimulated emission, exciton-polaritons, electron-hole plasma, three-photon absorption.

1. INTRODUCTION

Since its discovery in 2001 [1], ultraviolet laser action in ZnO nanowires has been experimentally investigated in several ways. Time-integrated measurements have been reported of the emission spectra of single nanowires [2-7] and of collections of nanowires [1, 6, 8-12]. In addition time-resolved experiments have been published [1, 8-10, 13-16]. Here Kerr-gated technique has served to measure stimulated emission from thin nanoneedles (20-60 nm) and other ZnO nanostructures with high time-resolution [9, 10]. Additional information on the charge carrier and lasing dynamics was obtained by time-resolved measurements of the second harmonic generation [13], by ultrafast 267-nm-pump 400-nm-optical-injection measurements [14], and by ultrafast pump-probe measurements in the range of 356 to 372 nm [15].

Although these experiments have revealed many properties of ZnO nanowires and of their laser action, the gain as a function of charge carrier density and wavelength has not yet been exhaustively investigated, nor the decay of the carrier density after a short pump pulse. Knowledge of the gain and the decay of the carrier density is very important for the design of devices based on nanowire lasing, but also for obtaining a correct theoretical description of the lasing mechanism in ZnO nanowires.

The literature on ZnO nanowire lasing does not provide a completely unambiguous picture of the lasing mechanisms and the corresponding thresholds, density regimes, and decay times. Is exciton-polariton lasing possible? What are the roles of inelastic scattering with excitons, with free carriers, and with the lattice in the laser action? How strong is the radiative decay compared to the non-radiative decay? Conclusive answers to these and related questions have to be found by comparing experimental results with detailed many-body theories [16, 17]. For this comparison it is a prerequisite to have experimental data on the gain and the carrier density as a function of time.

*m.a.m.versteegh@uu.nl

Ultrafast Phenomena in Semiconductors and Nanostructure Materials XIII,
edited by Kong-Thon Tsen, Jin-Joo Song, Markus Betz, Abdulhakem Y. Elezzabi,
Proc. of SPIE Vol. 7214, 721413 · © 2009 SPIE · CCC code: 0277-786X/09/$18 · doi: 10.1117/12.809250

Downloaded from SPIE Digital Library on 17 Apr 2012 to 131.180.82.147. Terms of Use: http://spiedl.org/terms

Here we present the results of ultrafast two-color pump-probe transmission experiments on a sample of ZnO nanowires. From these results we deduce the carrier density versus time following a pump pulse and the gain as a function of carrier density for several wavelengths. These relations can be used as starting point for a theoretical analysis.

It has been reported [19, 20] that the dispersion relation of exciton-polaritons exhibits a much larger longitudinal-transversal splitting in ZnO nanowires than in bulk ZnO. This observation indicates a much stronger light-matter interaction in the nanowires. The resulting stronger absorption and stronger stimulated emission have to be accounted for in the description of laser action.

In this paper we also present a novel method for the determination of exciton-polariton dispersion relations. This method relies on the use of an exciton-polariton ionizer pulse. We propose that employing this method light-matter interaction in ZnO nanowires can be further studied.

2. EXPERIMENTAL SECTION

We have used a sample of ZnO nanowires epitaxially grown on a sapphire surface, using the carbothermal reduction method with gold nanoparticles as catalysts [21]. It was made by Heng-Yu Li at the University of Utrecht. Fig. 1 is a SEM-image of our sample. The nanowires have a length of approximately 20 μm and a diameter of 100 to 500 nm. They cover 8 % of the surface of the sapphire crystal. As can be seen in Fig. 1, many nanowires of this sample touch each other.

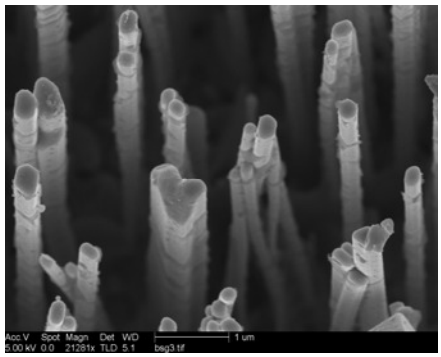

Fig. 1. SEM-image of our ZnO nanowire sample.

The pump-probe setup is illustrated in Fig. 2. Intense 120-fs 800-nm pulses were produced with a repetition rate of 1 kHz by an amplified Ti:sapphire laser (Hurricane, SpectraPhysics). The setup provides two options for the pump: the 800-nm pulses can be led through two BBO-crystals to produce 267-nm pulses, which are then focused onto the sample, or the 800-nm pulses can be directly focused onto the sample. The angle between the 267-nm pump beam and the nanowire axes is 17°, and for the 800-nm pump beam 30°.

The 267-nm pump directly excites electrons. Since the absorption coefficient above the band gap is 2×10^7 m^{-1} in bulk ZnO [22] and in ZnO thin films [23], this excitation is spatially inhomogeneous. The penetration depth is possibly even smaller in nanowires because of stronger light-matter interaction [19, 20]. Of course a small angle between the laser beam and the nanowire axis further reduces the excitation volume. After the excitation event some of the electrons will decay very fast. Others will diffuse over the nanowire on a timescale of a few picoseconds. Inhomogeneous excitation complicates the interpretation of the measurements.

Pumping with 800-nm pulses leads to excitation via two- and/or three-photon absorption [12, 24-26]. The absorption of 800-nm 120-fs pulses in ZnO nanowires is strong enough to reach the laser threshold [12]. In contrast to 267-nm excitation, 800-nm excitation is approximately homogeneous. This makes the analysis of the laser and carrier dynamics much simpler.

The probe wavelength in our setup is tunable. In a sapphire slab, intense 800-nm pulses undergo self-focusing and self-phase modulation, and white light is created. This white light allows measurements with probe wavelengths down to 450 nm, unfortunately not the most interesting wavelength range, since the laser action takes place near 385 nm. If a BBO crystal is inserted behind the sapphire crystal, sum-frequency is generated of 800-nm and one of the frequencies present in the white light pulse, depending on the orientation of the BBO crystal. In this way probe wavelengths around 400 nm can be generated. Between 380 and 420 nm the probe pulses are sufficiently strong to allow pump-probe measurements. The probe wavelength is measured by a spectrometer.

The probe is incident parallel to the nanowire axes and perpendicular to the sapphire substrate. The probe pulse is coupled in at the tops of the nanowires, guided through the wires, and coupled out again at the bottoms of the nanowires at the sapphire substrate. The transmission below band gap, measured with a solid angle of 0.5 sr, amounts to ~ 1 %. With this opening angle we catch most of the transmitted light. We estimate that ~ 10 % of the nanowires, weighed to the area of their tops, act as optical waveguides of the probe. The other nanowires are too thin, or have defects or improper

Downloaded from SPIE Digital Library on 17 Apr 2012 to 131.180.82.147. Terms of Use: http://spiedl.org/terms

orientations and shapes. As will be discussed in section 3.2, we estimate the fraction of probe light that reaches the sapphire without guiding through the ZnO wires to be 40-50 %. This has two causes: 1) Multiple scattering at the nanowires, at lumps of ZnO at the sapphire substrate and at gold nanoparticles lying between the nanowires at the sapphire substrate. 2) Absorption of probe light in the gold nanoparticles and in ZnO nanowires and ZnO lumps, especially in defects.

The probe light that is transmitted through the sample is collected by a lens and detected by a photodiode. A grating and a chopper in combination with a lock-in amplifier are used to separate the probe light from the pump light and the photoluminescence. With a microscope in combination with a CCD camera we locate the pump and probe spots on the sample. The probe spot is small enough to ensure the pump fluence to be approximately constant over the probe spot.

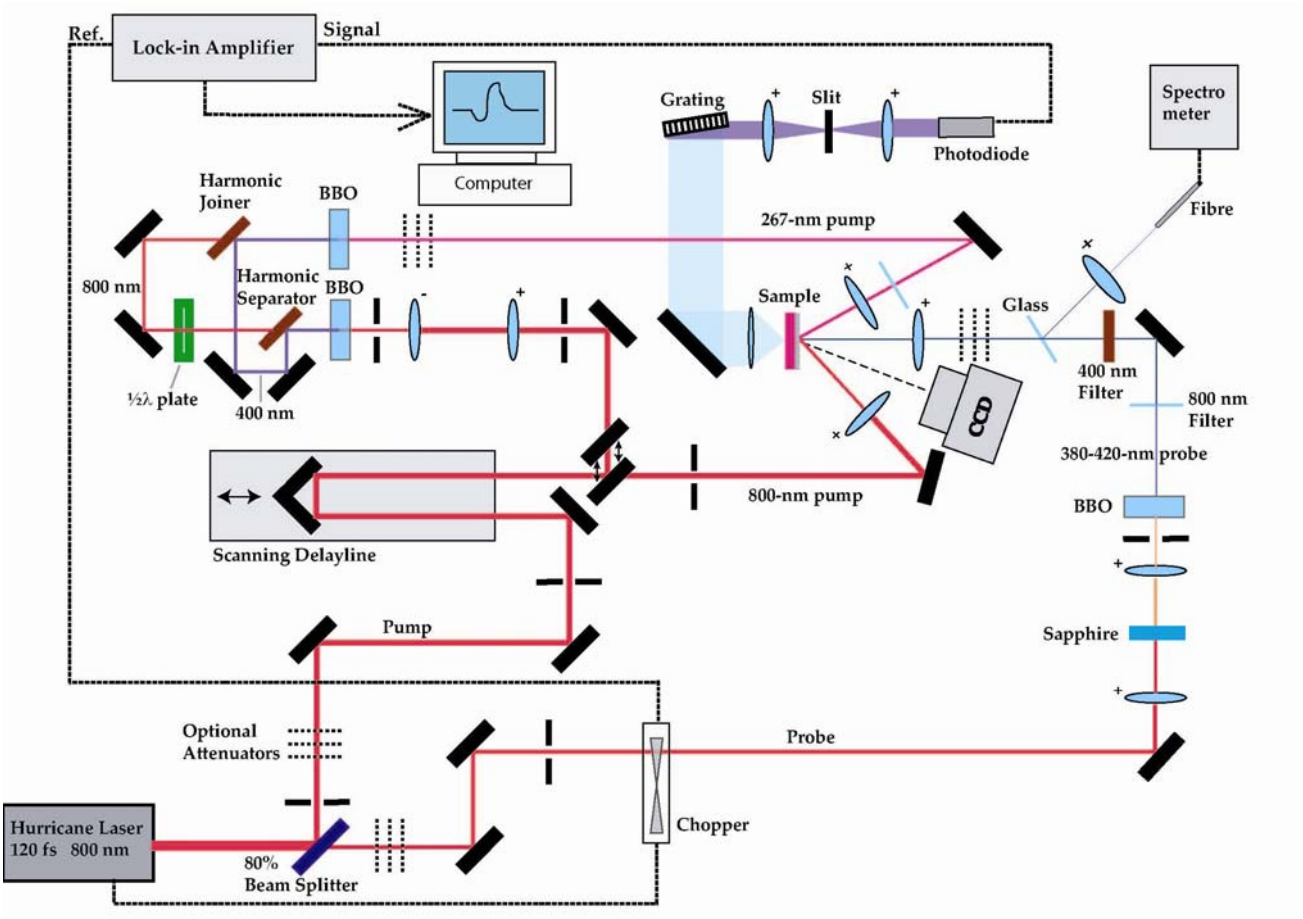

Fig. 2. The ultrafast pump-probe setup. For the pump there are two options: after the scanning delay line the 800-nm pump pulses can be directly focused onto the nanowire sample, or a mirror can be moved into the beam, sending it through two BBO crystals, after which the resulting 267-nm pulses are led through an interference filter and focused onto the sample. As probe the white light ($\lambda > 450$ nm) that is generated in the sapphire can be used, or a BBO crystal can be placed behind the sapphire with which probe pulses are made with a wavelength in the range of 380 to 420 nm and a linewidth (FWHM) of 2 nm.

Downloaded from SPIE Digital Library on 17 Apr 2012 to 131.180.82.147. Terms of Use: http://spiedl.org/terms

3. RESULTS AND DISCUSSION

3.1 Pump-probe results

The results of the pump-probe measurements with the 800-nm pump (homogeneous excitation) for four different probe wavelengths are shown in Fig. 3. The change in transmission through the nanowire sample is normalized to the transmission in absence of the pump, as a function of the time delay between pump and probe. The graphs have two clear features: a dip (a decrease of the transmission of the probe) and a peak (an increase in the transmission of the probe). The bottom of the dip defines $t = 0$. At $t = 0$, pump and probe are simultaneously in the nanowires, and interact with each other, as will be explained in section 3.2.

The peak is the result of amplification of the probe by stimulated emission. The stimulated emission is the strongest at 385 nm (Fig. 3d), where the probe signal increases up to a factor 34. Amplification is observed for all four probe wavelengths for pump fluences exceeding 150 J/m^2. As the delay between pump and probe is increased, the amplification decreases due to decay of the charge carrier density. The results clearly show that the higher the pump fluence, that is the higher the carrier density, the stronger the amplification and the faster the decay.

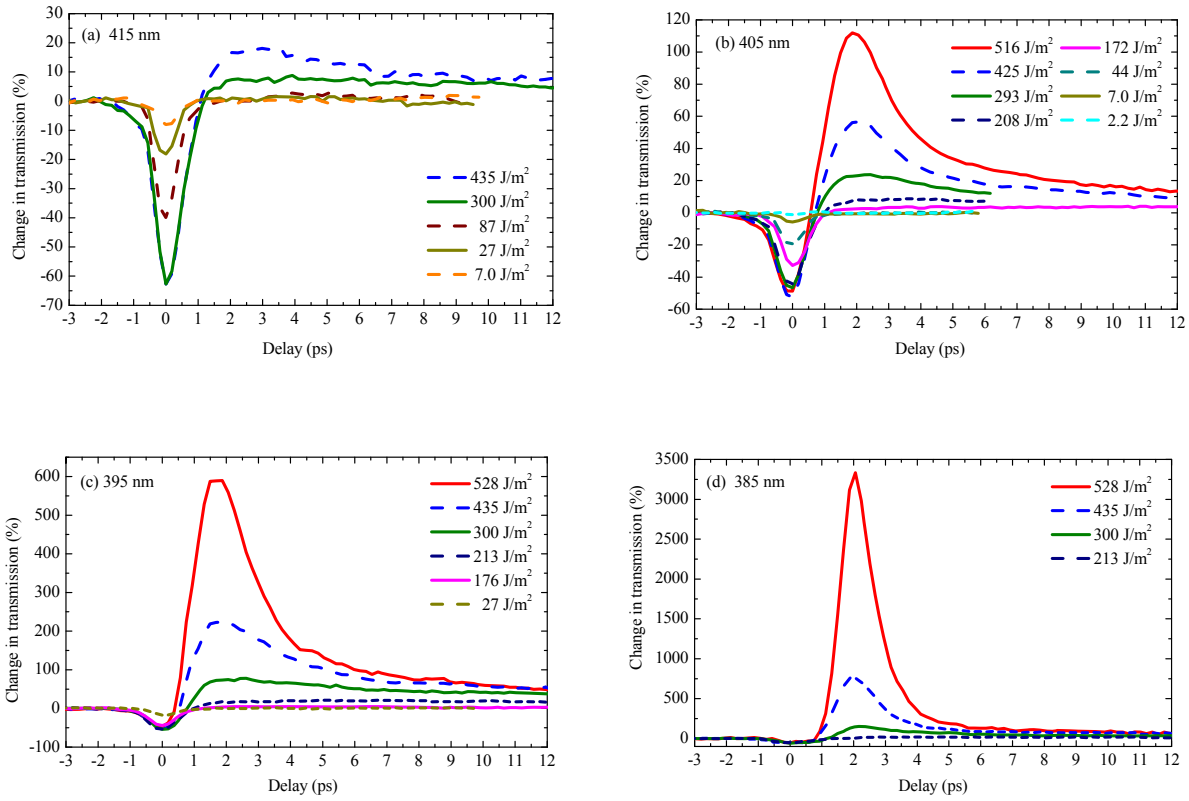

Fig. 3. Results of the 800-nm pump-probe transmission measurements on the ZnO nanowires for several different pump fluences and probe wavelengths. The probe wavelengths were (a) 415 nm, (b) 405 nm, (c) 395 nm and (d) 385 nm.

Results for a 395-nm probe for a longer delay are shown in Fig. 4. We observe a slowing down of the decay for smaller carrier densities.

In Fig. 5 results are shown for a 267-nm pump and a 400-nm probe. Again, we observe a dip and a peak. The amplification remains quite constant at 3 - 4 % between pump fluences of 2 and 30 J/m^2. At 30 J/m^2 decay speeds up and at 35 J/m^2 the amplification is much stronger, signifying threshold behavior.

Downloaded from SPIE Digital Library on 17 Apr 2012 to 131.180.82.147. Terms of Use: http://spiedl.org/terms

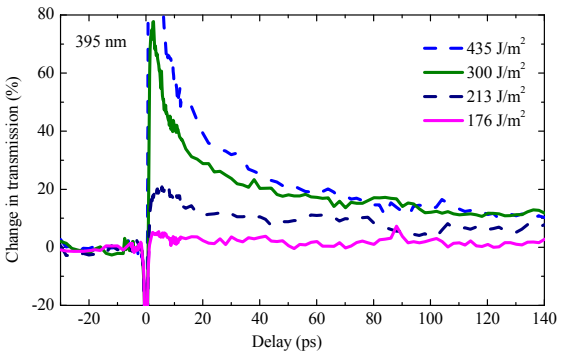

Fig. 4. 800-nm pump 395-nm probe results.

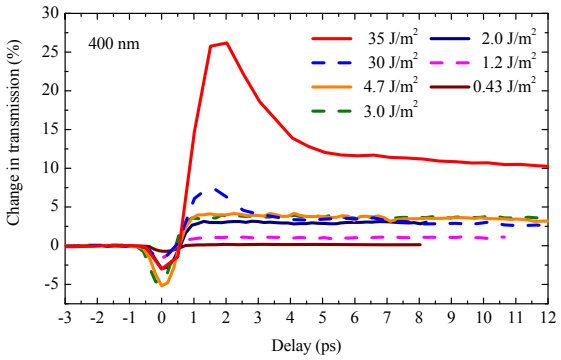

Fig. 5. 267-nm pump 400-nm probe results.

3.2 Exciton-polariton ionizer

In all pump-probe measurements with the probe wavelength in the range of 385 to 415 nm, a fast dip appears in the transmission signal. In case of 800-nm pumping (Fig. 3 and 4) the depth is linearly dependent on pump fluence, until it saturates at 50 to 60 %. The depth does not significantly depend on the probe wavelength. The width of the dip, however, does depend on the probe wavelength and changes from 0.89 ps at 415 nm to 1.38 ps at 385 nm.

The dip is caused by switching off of the probe waveguiding when the pump meets the probe in the wire. When the probe pulse moves through a nanowire, it is in the form of an exciton-polariton wave packet. The 800-nm pump pulse moves faster than the probe exciton-polariton wave packet. When the intense pump catches up with the probe, it ionizes the exciton-polaritons. This effect explains the rapid decrease in transmission of the probe. The dip commences when the delay between probe and pump is such that the pump just catches up with the probe at the bottom of the nanowires, and ends when the pump meets the probe at the top of the nanowires. Apart from the pulse durations of pump and probe, the width of the dip is determined by the velocity of the probe, the velocity of the pump, and the length of the wires.

As can be seen from Table 1, the width increases as the probe wavelength approaches the exciton resonance at 375 nm (3.31 eV), indicating that the exciton-polaritons close to the resonance move slower. In principle, from the width of the dip the group velocity of the exciton-polaritons, and hence the exciton-polariton dispersion relation can be easily calculated. For ZnO nanowires a determination of the exciton-polariton dispersion relation is particularly interesting, because of the enhancement of the light-matter interaction, as reported in Ref. [19, 20], which should be visible in the dispersion relation. Since the shape of nanowires makes it very difficult to perform a reflection experiment on them, using an exciton-polariton ionizer seems to be an interesting method to measure the dispersion relation.

The saturation of the dip suggests that, in the absence of a pump, 50 to 60 % of the detected probe light manages to travel through the nanowires. The remaining 40 to 50 % diffuses between the nanowires to the sapphire.

Table 1. Width of the dip.

Probe wavelength	Width of the dip (FWHM)
415 nm	0.89 ps
405 nm	0.96 ps
395 nm	1.07 ps
390 nm	1.20 ps
385 nm	1.38 ps

Also the 267-nm pump can act as an exciton-polariton ionizer (Fig. 5). However, the resulting dip in the transmission has a maximal depth of 5 to 8 %. This implies that the 267-nm pump ionizes only 10 to 15 % of the probe exciton-polaritons, consistent with the small penetration depth of 267-nm pump light.

The dip in the pump-probe signal had been observed earlier in experiments on ZnO nanorods [15] and nanowires [14] and on GaN thin films [27]. In Ref. [15, 27] the dip is correctly explained as a result of excitonic enhancement of 2PA.

Downloaded from SPIE Digital Library on 17 Apr 2012 to 131.180.82.147. Terms of Use: http://spiedl.org/terms

3.3 The carrier density and its decay

From the pump-probe results we deduce the time-evolution of the carrier density and the gain as a function of carrier density for different wavelengths. For the 800-nm pump measurements this is more straightforward, since the 800-nm excitation leads to a homogeneous carrier density, and pump fluence can be directly related to carrier density. Therefore we will concentrate on the analysis of the 800-nm results.

In order to compute the carrier densities, we have to consider absorption of 800-nm light in ZnO. The energy of 800-nm photons (1.55 eV) is less than half the energy of an exciton in the ground state, which is 3.31 eV. Therefore it is to be expected that absorption of 800-nm light takes place via three-photon absorption (3PA). For 120-fs pulses at fluences below 50 J/m^2, Z-scan transmission measurements on a bulk ZnO crystal [24] show that two-photon absorption (2PA) dominates at wavelengths up to 770 nm and 3PA dominates at longer wavelengths. For higher fluences where we have detected amplification, 3PA must surely be much stronger than 2PA. A 3PA coefficient of $(1.0 \pm 0.2) \times 10^{-26}$ m^3/W^2 for 800-nm light in bulk ZnO has been reported [24].

Photoluminescence experiments on bulk ZnO [25] show that in case of pumping with 800-nm 80-fs laser pulses the intensity of the UV photoluminescence is proportional to the fluence to the power 3.8. In case of 700-nm and 720-nm pumping it is proportional to the fluence to the power 2.5. This supports the idea of carrier generation via 3PA in case of 800-nm pumping and via 2PA in case of 700-nm and 720-nm pumping.

We have performed photoluminescence measurements on the nanowires with 800-nm pump pulses. The radiation from the nanowires can be divided into three parts: UV emission, second harmonic generation at 400 nm and visible luminescence from deep centers. Results for the fluence dependences are shown in Fig. 6. For the UV emission we find that it is proportional to the fluence to the power 3.7 ± 0.3. For the visible deep center luminescence we find a power 2.0 ± 0.2, prior to saturation at a fluence of 300 J/m^2. The supralinear dependence of the UV luminescence emission on the carrier density is explained by the fact that part of the UV emission is caused by inelastic exciton-exciton collisions, exciton-carrier collisions and carrier-carrier collisions. Apparently, radiative decay gains in importance for increased exciton and/or carrier densities.

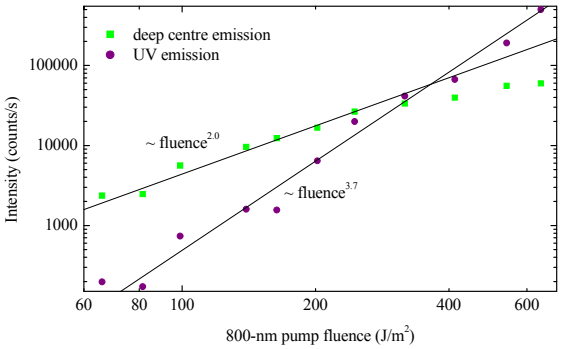

Fig. 6. Fluence dependence of the UV and deep center emission from the nanowires for 800-nm excitation.

From the dependence of the UV-emission on the 800-nm pump fluence we conclude that 3PA governs carrier generation in our sample. Our results are similar to the bulk results of Ref. [25]. We note that in Ref. [12, 26] a quadratic dependence of the UV-emission from ZnO nanowires on the 800-nm pump fluence is reported. The difference with our results might be due to a difference in the nanowire samples.

The calculation of the carrier density and its time evolution from the pump-probe results of Fig. 3 is done in two steps.

The first step is the calculation of the carrier densities at t = 2.0 ps. As can be seen in Fig. 3, this is the time at which for all pump fluences and probe wavelengths, the amplification is maximal. We take the following assumptions and approximations: 1) The 3PA coefficient for the ZnO nanowires is equal to the coefficient of 1.0×10^{-26} m^3/W^2, found for bulk ZnO [24]. If indeed light-matter interaction in nanowires is stronger than in bulk ZnO, then this assumption could be wrong. 2) 89 % of the 800-nm light that hits the nanowires, enters. 3) The pump pulses have a Gaussian temporal profile with a standard deviation of 60 fs. 4) Extinction of the pump pulses due to 1PA, 2PA and 3PA is negligible. With these assumptions we derive the following relation between the pump fluence f and the carrier density n that is present in the material just after the pump pulse has passed:

$$n(f) = \int_{-\infty}^{\infty} \frac{\gamma}{3\hbar\omega} \left(\frac{0.89 f}{\sqrt{2\pi} d} e^{-\frac{t^2}{2d^2}} \right)^3 dt \,, \qquad (1)$$

Downloaded from SPIE Digital Library on 17 Apr 2012 to 131.180.82.147. Terms of Use: http://spiedl.org/terms

with $\gamma = 1.0 \times 10^{-26}$ m^3/W^2, $d = 60$ fs and $\hbar\omega = 1.55$ eV. The nanowires are long compared to the average distance between the wires and the angle between the 800-nm pump and the wires is 30°, so only the top ~ 4 μm of the wires can be reached directly by the pump. However, we think that by transmission, scattering and waveguiding 800-nm pump pulses reach the lower parts of the wires very well, so that the following assumption is justified: 5) The carrier density is in the entire wire given by Eq. (1). Note that for 267-nm pumping such an assumption cannot be made because of strong absorption. We finally use the following approximation: 6) We neglect the decay of the carrier density before $t = 2.0$ ps. This approximation overestimates the carrier density at $t = 2.0$ ps. Under these reasonable assumptions and approximations, the carrier density at $t = 2.0$ ps in the entire nanowire is given by Eq. (1).

The second step is the calculation of the carrier density after $t = 2.0$ ps. We assume: 7) The change in transmission of the probe only depends on the carrier density. If we apply this assumption on Fig. 3b for example, then we conclude that for a pump fluence of 516 J/m^2 the carrier density at $t = 3.5$ ps is equal to the carrier density at $t = 2.0$ ps for a fluence of 425 J/m^2, and that the carrier density at $t = 7.1$ ps is equal to the carrier density at $t = 2.0$ ps for a fluence of 293 J/m^2. In this way carrier densities after $t = 2.0$ ps can be related to carrier densities at $t = 2.0$ ps. To the measurement points at $t = 2.0$ ps for each probe wavelength a function can be fit that gives the relation between the change in transmission and the carrier density, according to Eq. (1). Using this function, vertical axes of change in transmission can be transformed into axes of carrier density. Results for 385-nm and 405-nm probes are presented in Fig. 7 for indicated fluences. The traces are quite similar, as they should, because the carrier density does not depend on the probe wavelength selected.

We observe in Fig. 7 a fast decay (decay time ~ 1.5 ps) for carrier densities higher than ~ 10^{25} m^{-3}. For these densities the electrons and holes form a degenerate EHP [28]. The distance between the quasi-Fermi levels of electrons and holes exceeds the renormalized band gap. As soon as the density has decreased to values between 5×10^{24} and 1×10^{25} m^{-3}, the EHP becomes classical and the decay slows down. In all our dynamical measurements where amplification is detected, the density is higher than the Mott density, which is 5×10^{23} m^{-3} [28], so excitons are not involved.

These results of the decay of the carrier density in ZnO nanowires are well compatible with the reported results of measurements of transient second harmonic generation [13] and lasing dynamics [9, 10, 14]. Also THz measurements on bulk ZnO showed a fast (~ 1.5 ps) decay of the carrier density of an electron-hole plasma [29].

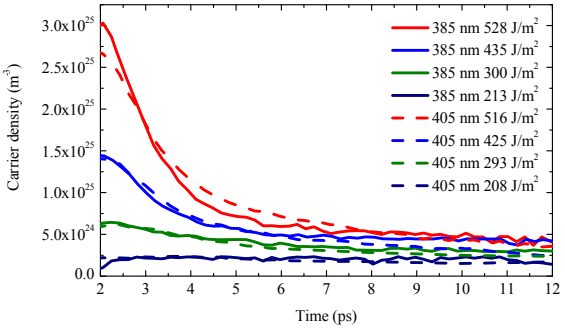

Fig. 7. The carrier density after an 800-nm pump pulse vs. time, calculated from pump-probe results of Fig. 3b and 3d.

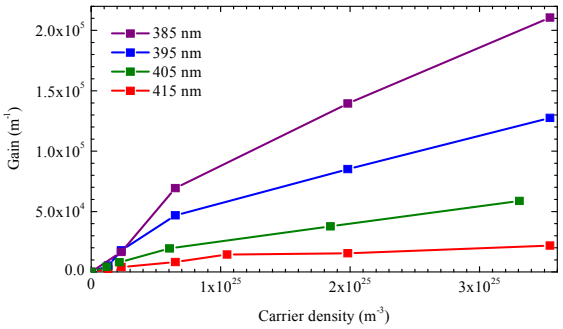

Fig. 8. The gain of the probe light in the ZnO nanowires as a function of carrier density for four probe wavelengths.

3.4 Gain

From the increase in transmission (Fig. 3) the gain coefficient can readily be calculated. We assume an exponential increase of the probe intensity through the 20 μm long nanowires in case of 800-nm pumping. In the calculation of the gain, we neglect all losses of the probe intensity inside the nanowires and we assume that, in the absence of a pump, 50 % of the detected probe light has been guided through the nanowires. The remaining 50 % reaches the sapphire by scattering and diffusion without waveguiding.

Downloaded from SPIE Digital Library on 17 Apr 2012 to 131.180.82.147. Terms of Use: http://spiedl.org/terms

The result is given in Fig. 8. As can be seen, for densities below ~ 10^{25} m^{-3} the gain linearly increases with the carrier density, with steeper slopes for probe wavelengths closer to the resonance. For densities higher than 10^{25} m^{-3}, when the electron-hole plasma is degenerate, the slope is less. Phase space filling, band gap renormalization and screening play a significant role here. At low carrier densities (but higher than the Mott density) the gain mechanism involves inelastic carrier-carrier collisions and/or emission of phonon-plasmon mixed state quanta [28]. Amplification of the probe by direct recombination becomes possible when the band gap shrinks to an energy level lower than the probe energy. From Ref. [17] it can be calculated that for a probe wavelength of 385 nm, the band gap is reached at 4×10^{24} m^{-3}, for a wavelength of 395 nm, it is reached at 1×10^{25} m^{-3}, for 405 nm at 2×10^{25} m^{-3}, and for 415 nm at 4×10^{25} m^{-3}.

In order to find the required gain coefficient for lasing, one has to compute the reflection constants at the ZnO-sapphire and at the ZnO-air interfaces. This is not trivial, since one has to take into account that part of the electromagnetic wave is evanescent [30] and that the index of refraction is modified by both the high carrier density [18, ch. 15] and small dimensions of the nanowire, leading to a larger longitudinal-transversal splitting [19, 20]. The presence of gold at the sapphire surface could enhance the reflection [5]. Not all nanowires show laser action and the laser threshold may vary for different nanowires [4, 13].

4. CONCLUSION

We performed ultrafast two-color pump-probe measurements on ZnO nanowires. Incident 800-nm pump pulses gave rise to a homogeneous carrier density via 3PA, 267-nm pump pulses led to an inhomogeneous density via 1PA. The probe with a linewidth of 2 nm was tuned between 385 and 415 nm. The results show a rapid dip when pump and probe are simultaneously in the nanowires and amplification of the probe when it is delayed with respect to the pump. The dip is caused by the ionization of the probe exciton-polaritons by the pump and can be used to study the dispersion relation. From the measured amplification we have deduced the time-evolution of the carrier density that was created by the pump and the gain coefficient as a function of carrier density for several wavelengths. When the density is higher than ~ 10^{25} m^{-3}, the decay is fast (~ 1.5 ps). It slows down when the density has decreased to values between 5×10^{24} and 1×10^{25} m^{-3}. We note that the densities for which the decay is fast, coincide with the densities for which the electron-hole plasma is degenerate. It is tempting to conclude that the fast decay is caused by amplification by direct recombination and possibly lasing. However, we feel that further work is needed to be able to draw conclusions about the laser mechanism in ZnO nanowires.

AKNOWLEDGEMENTS

We thank Cees R. de Kok and Paul Jurrius for their technical support. We thank Heng-Yu Li for making the nanowire samples.

REFERENCES

[1] Huang, M.H., Mao, S., Feick, H., Yan, H., Wu, Y., Kind, H., Weber, E., Russo, R., and Yang, P., "Room-Temperature Ultraviolet Nanowire Nanolasers", Science 292, 1897-1899 (2001).

[2] Johnson, J.C., Yan, H., Schaller, R.D., Haber, L.H., Saykally, R.J., and Yang, P., "Single Nanowire Lasers", J. Phys. Chem. B 105, 11387-11390 (2001).

[3] Johnson, J.C., Yan, H., Yang, P., and Saykally, R.J., "Optical Cavity Effects in ZnO Nanowire Lasers and Waveguides", J. Phys. Chem. B 107, 8816-8828 (2003).

[4] van Vugt, L.K., Rühle, S., and Vanmaekelbergh, D., "Phase-Correlated Nondirectional Laser Emission from the End Facets of a ZnO Nanowire", Nano Lett. 6(12), 2707-2711 (2006).

[5] Hauschild, R., Lange, H., Priller, H., Klingshirn, C., Kling, R. Waag, A., Fan, H.J., Zacharias, M., and Kalt, H., "Stimulated emission from ZnO nanorods", Phys. Stat. Sol. (b) 243(4), 853-857 (2006).

Downloaded from SPIE Digital Library on 17 Apr 2012 to 131.180.82.147. Terms of Use: http://spiedl.org/terms

[6] Zhou, H., Wissinger, M., Fallert, J., Hauschild, R., Stelzl, F., Klingshirn, C. and Kalt, H., "Ordered, uniform-sized ZnO nanolaser arrays", Appl. Phys. Lett. 91, 181112 (2007).
[7] Zimmler, M.A., Bao, J., Capasso, F., Müller, S., and Ronning, C., "Laser action in nanowires: Observation of the transition from amplified spontaneous emission to laser oscillation", Appl. Phys. Lett. 93, 051101 (2008).
[8] Choy, J.-H., Jang, E.-S., Won, J.-H., Chung, J.-H., Jang, D.-J., and Kim, Y.-W., "Soft Solution Route to Directionally Grown ZnO Nanorod Arrays on Si Wafer; Room-Temperature Ultraviolet Laser", Adv. Mater. 15(22), 1911-1914 (2003).
[9] Kwok, W.M., Djurišić, A.B., Leung, Y.H., Chan, W.K., and Phillips, D.L, "Time-resolved photoluminescence study of the stimulated emission in ZnO nanoneedles", Appl. Phys. Lett. 87, 093108 (2005).
[10] Djurišić, A.B., Kwok, W.M., Leung, Y.H., Phillips, D.L., and Chan, W.K., "Stimulated Emission in ZnO Nanostructures: A Time-Resolved Study", J. Phys. Chem. B 109, 19228-19233 (2005).
[11] Hsu, H.-C., Wu, C.-Y. and Hsieh, W.-F., "Stimulated emission and lasing of random-growth oriented ZnO nanowires", J. Appl. Phys. 97, 064315 (2005).
[12] Zhang, C.F., Dong, Z.W., You, G.J., Qian, S.X., and Deng, H., "Multiphoton route to ZnO nanowire lasers", Opt. Lett. 31(22), 3345-3347 (2006).
[13] Johnson, J.C., Knutsen, K.P., Yan, H., Law, M., Zhang, Y., Yang, P., and Saykally, R.J., "Ultrafast Carrier Dynamics in Single ZnO Nanowire and Nanoribbon Lasers", Nano Lett. 4(2), 197-204 (2004).
[14] Song, J.K., Szarko, J.M., Leone, S.R., Li, S., and Zhao, Y., "Ultrafast Wavelength-Dependent Lasing-Time Dynamics in Single ZnO Nanotetrapod and Nanowire Lasers", J. Phys. Chem. B 109, 15749-15753 (2005).
[15] Sun, C.-K., Sun, S.-Z., Lin, K.-H., Zhang, K.Y.-J., Liu, H.-L., Liu, S.-C., and Wu, J.-J., "Ultrafast carrier dynamics in ZnO nanorods", Appl. Phys. Lett. 87, 023106 (2005).
[16] Fallert, J., Stelz, F., Zhou, H., Reiser, A., Thonke, K., Sauer, R., Klingshirn, C, and Kalt, H., "Lasing dynamics in single ZnO nanorods", Opt. Express 16(2), 1125-1131 (2008).
[17] Inagaki, T.J. and Aihara, M., "Many-body theory for luminescence spectra in high-density electron-hole systems", Phys. Rev. B 65, 205204 (2002).
[18] Haug, H. and Koch, S.W., [Quantum Theory of the Optical and Electronic Properties of Semiconductors], fourth edition, World Scientific, Singapore (2004).
[19] van Vugt, L.K., Rühle, S., Ravindran, P., Gerritsen, H.C., Kuipers, L, and Vanmaekelbergh, D., "Exciton Polaritons Confined in a ZnO Nanowire Cavity", Phys. Rev. Lett. 97, 147401 (2006).
[20] Rühle, S., van Vugt, L.K., Li, H.-Y., Keizer, N.A., Kuipers, L., and Vanmaekelbergh, D. "Nature of Sub-Band Gap Luminescent Eigenmodes in a ZnO Nanowire", Nano Lett. 8(1), 119-123 (2008).
[21] Prasanth, R., van Vugt, L.K., Vanmaekelbergh, D.A.M., and Gerritsen, H.C., "Resonance enhancement of optical second harmonic generation in a ZnO nanowire", Appl. Phys. Lett. 88, 181501 (2006).
[22] Jellison, G.E., Jr. and Boatner, L.A., "Optical functions of uniaxial ZnO determined by generalized ellipsometry", Phys. Rev. B 58(7), 3586-3589 (1998).
[23] Muth, J.F., Kolbas, R.M., Sharma, A.K., Oktyabrsky, S., and Narayan, J., "Excitonic structure and absorption coefficient measurements of ZnO single crystal epitaxial films deposited by pulsed laser deposition", J. Appl. Phys. 85(11), 7884-7887 (1999).
[24] He, J., Qu, Y., Li, H., Mi, J., and Wei, J., "Three-photon absorption in ZnO and ZnS crystals", Opt. Express 13(23), 9235-9247 (2005).
[25] Dai, D.C., Xu, S.J., Shi, S.L., Xie, M.H., and Che, C.M., "Efficient multiphoton-absorption-induced luminescence in single-crystalline ZnO at room temperature", Opt. Lett. 30(24), 3377-3379 (2005).
[26] Zhang, C.F., Dong, Z.W., You, G.J., Zhu, R.Y., Qian, S.X., Deng, H., Cheng, H., and Wang, J.C., "Femtosecond pulse excited two-photon photoluminescence and second harmonic generation in ZnO nanowires", Appl. Phys. Lett. 89, 042117 (2006).
[27] Lin, K.-H., Chern, G.-W., Huang, Y.-C., Keller, S., DenBaars, S.P., and Sun, C.-K., "Observation of hugh nonlinear absorption enhancement near exciton resonance in GaN", Appl. Phys. Lett. 83(15), 3087-3089 (2003).
[28] Klingshirn, C., Hauschild, R., Fallert, J., and Kalt, H., "Room-temperature stimulated emission of ZnO: Alternatives to excitonic lasing", Phys. Rev. B 75, 115203 (2007).
[29] Hendry, E., Koeberg, M., and Bonn, M., "Exciton and electron-hole plasma formation dynamics in ZnO", Phys. Rev. B 76, 045214 (2007).
[30] Voss, T., Svacha, G.T., Mazur, E., Müller, S., Ronning, C., Konjhodzic, D., and Marlow, F., "High-Order Waveguide Modes in ZnO Nanowires", Nano Lett. 7(12), 3675-3680 (2007).

Downloaded from SPIE Digital Library on 17 Apr 2012 to 131.180.82.147. Terms of Use: http://spiedl.org/terms